CM² MAGAZINE

第 34 期

南方科技大学海洋磁学中心主编

创刊词

海洋是生命的摇篮，是文明的纽带。地球上最早的生命诞生于海洋，海洋里的生命最终进化成了人类，人类的文化融合又通过海洋得以实现。人因海而兴。

人类对海洋的探索从未停止。从远古时代美丽的神话传说，到麦哲伦的全球航行，再到现代对大洋的科学钻探计划，海洋逐渐从人类敬畏崇拜幻想的精神寄托演变成可以开发利用与科学研究的客观存在。其中，上个世纪与太空探索同步发展的大洋科学钻探计划将人类对海洋的认知推向了崭新的纬度：深海（deep sea）与深时（deep time）。大洋钻探计划让人类知道，奔流不息的大海之下，埋藏的却是亿万年的地球历史。它们记录了地球板块的运动，从而使板块构造学说得到证实；它们记录了地球环境的演变，从而让古海洋学方兴未艾。

在探索海洋的悠久历史中，从大航海时代的导航，到大洋钻探计划中不可或缺的磁性地层学，磁学发挥了不可替代的作用。这不是偶然，因为从微观到宏观，磁性是最基本的物理属性之一，可以说，万物皆有磁性。基于课题组的学科背景和对海洋的理解，我们对海洋的探索以磁学为主要手段，海洋磁学中心因此而生。

海洋磁学中心，简称 CM^2，一为其全名“Centre for Marine Magnetism”的缩写，另者恰与爱因斯坦著名的质能方程 $E = MC^2$ 对称，借以表达我们对科学巨匠的敬仰和对科学的不懈追求。

然而科学从来不是单打独斗的产物。我们以磁学为研究海洋的主攻利器，但绝不仅限于磁学。凡与磁学相关的领域均是我们关注的重点。为了跟踪反映国内外地球科学特别是与磁学有关的地球科学领域的最新研究进展，海洋磁学中心特地主办 CM^2 Magazine，以期与各位地球科学工作者相互交流学习、合作共进！

“海洋孕育了生命，联通了世界，促进了发展”。 21 世纪是海洋科学的时代，由陆向海，让我们携手迈进中国海洋科学的黄金时代

目 录

第 24 章　DRM 倾角变浅

还有一类样品我们必须提及，那就是黄土、石笋、珊瑚等介质。黄土的压实很小，所以它不可能通过正常的 Lock-in 过程来锁定 DRM，更多的是胶结过程。同理，石笋和珊瑚也不可能是传统的 Lock-in 过程。石笋靠的是 CaCO3 结晶胶结，所以它记录的磁场方向就较为准确。靠压实过程锁定的 DRM，其倾角经常会变浅。

DRM 倾角变浅是一个广泛存在的现象。我们想象一个极端情况，如果把一个沉积层都压成扁片了，所有的磁性矿物颗粒的长轴都会在水平面上分布，其倾角肯定会向水平方向偏转。

通过实验我们得知，在小倾角（<10°）或者大倾角（>80°）范围，倾角变化误差较小。在 45°左右，倾角变浅的现象非常明显。通过经验公式，我们得出：

tan(I 观测)= f * tan(I 真实)，

在这里 f 是一个常量系数（不代表频率），0 < f < 1。

如果我们能够通过实验得到这个系数，通过矫正就可以把真实倾角给恢复。

第一种思路是利用 AMS。在压实过程中，除了 DRM 的倾角会变浅，样品的 AMS 参数也会变化，比如 P 值会增大等。如果我们能够建立 AMS 参数和 f 之间的关系，就能通过 AMS 参数计算 f。

除了 AMS，其它参数也有各向异性。比如 IRM 和 ARM，相应的各向异性叫做 AIRM 和 AARM。对于剩磁来讲，AARM 和 AIRM 可能会比 AMS 更相关。但是和 AMS 比起来，AARM 和 AIRM 的测量方式会复杂些。

第二种方式就复杂了，利用了古地磁方向的统计特征。

我们知道，地磁场的极并不总是指向正南正北，而是围绕着南北方向打圈圈。在统计意义上，比如把几个百万年的极点统计一下，就会发现这个统计的极点才指向正南正北，这个模型叫做 GAD 模型。

由于极点的绕动，在地球上任何一个位置上的倾角和偏角也遵循一定的分布（椭圆形分布）。根据现今地磁场卫星磁测结果，我们发现，越靠近赤道，这个椭圆分布的拉长度（Elongation）就越高，越靠近高纬度，这个分布就接近圆形，拉长度变低。

Lisa Tauxe 教授首先建立了一个拉长度和纬度变化的标准曲线，以它为模板，和实际数据去对比。

沉积物经过压实后，其倾角会变浅，其相应的倾角和偏角的分布拉长度也会变化。于是，利用 tan (I 观测) = f * tan (I 真实)这个关系式，寻找一个合适的 f 值，使得改正的拉长度和理论拉长度一致，这样我们就认为寻找到了一个合理的 f 值，并用它来统一矫正观测的倾角值。这个方法叫做 E-I 矫正法。

火山岩记录 TRM 没有压实作用，倾角不会变浅。所以如果碰到沉积层和火山岩互层时，就可以把火山岩记录的倾角和沉积层记录的倾角相互对比，如果二者的值相似，就说明倾角变浅现象不明显。否则，就可以用火山岩的数据对沉积层数据进行矫正。

这看起来很合理，但是我们知道火山岩是间断性喷发的，记录的是瞬时信息。地磁场本身就是在变化的，瞬时信息会有偏差，所以，到目前为止，这种相比较的方法并没有完全解决这个问题。

还有一种方法，那就是把野外采集回来的沉积物，在实验室磁场环境中重新进行沉积实验模拟。尽管存在着这样或者那样的环境不一致性，通过沉积实验，改变外场的磁化方向，做一条 I 观测和 I 真实之间的相关曲线，把 f 值拟合出来。尽管实验量很大，但是值得去做。

总之，和地学相关的数据都很复杂，因为所有信息都是被介质记录的，地质记录过程就是一个滤波器，或多或少都会对原有信息进行改造。因此，我们尽可能用多种方法对同一现象进行研究，如果多方法的结果有可比性，就会增加数据解释的合理性。

比如，我们可以同时做 AMS 校正和 E-I 校正，看校正后能否得到一致的结果。如果有火山岩数据，可三者同时对比。

有人会问，为什么要对沉积物的地磁倾角进行校正？

古地磁学家通过地磁倾角来计算所处地方的古纬度。如果倾角变浅了，那么计算出来的古纬度就偏低。本来板块处在中纬度，倾角变浅后，就会把板块安排到低纬度，这在板块运动和古地理重建时，会产生很大的偏差。

CM2 研究进展

西太平洋锰结核微生物矿化研究及对生物地球化学循环和锰结核成矿的指示意义

深海锰结核因富含 Cu、Co、Ni、稀土等金属元素而具有重要的经济价值，因生长缓慢而记录了长时间尺度的古环境变化。微生物活动常常被认为对锰结核成矿具有重要意义。然而，目前微生物与锰结核生长的关系仍不清楚，微生物矿化作用对锰结核成矿的贡献到底有多大亦是未知。

本研究对取自西太平洋的锰结核进行了微生物群落、元素分布、矿物组成和孔隙结构分析。研究发现锰结核中存在大量细菌与古菌，其中一些种类可能具有铁还原、锰氧化和氨厌氧氧化功能。锰结核中还观察到大量锰氧化菌趋磁菌矿化形成的锰氧化菌化石和磁小体化石。此外，相较于内部老层位锰结核年轻层位中具有更显著的生物地球化学反应，锰结核内的微米与纳米结构提供了有利于微生物生长的微环境和营养运输通道，并且促进锰结核的生长，同时表明微生物系统与锰结核生长之间的相互依赖关系。这些结果对探究底层海水与沉积物之间的生物地球化学循环具有重要意义。

通过对磁小体化石进行磁学性质和形态特征分析，我们估算生物磁铁矿在锰结核中的含量，并进一步推算锰氧化菌的含量。结果暗示微生物矿化作用对锰结核形成具有重要意义，在极低初级生产力海域却有如此大规模的微生物矿化，意味着锰结核形成是深海环境中生物地球化学循环很重要的一部分。

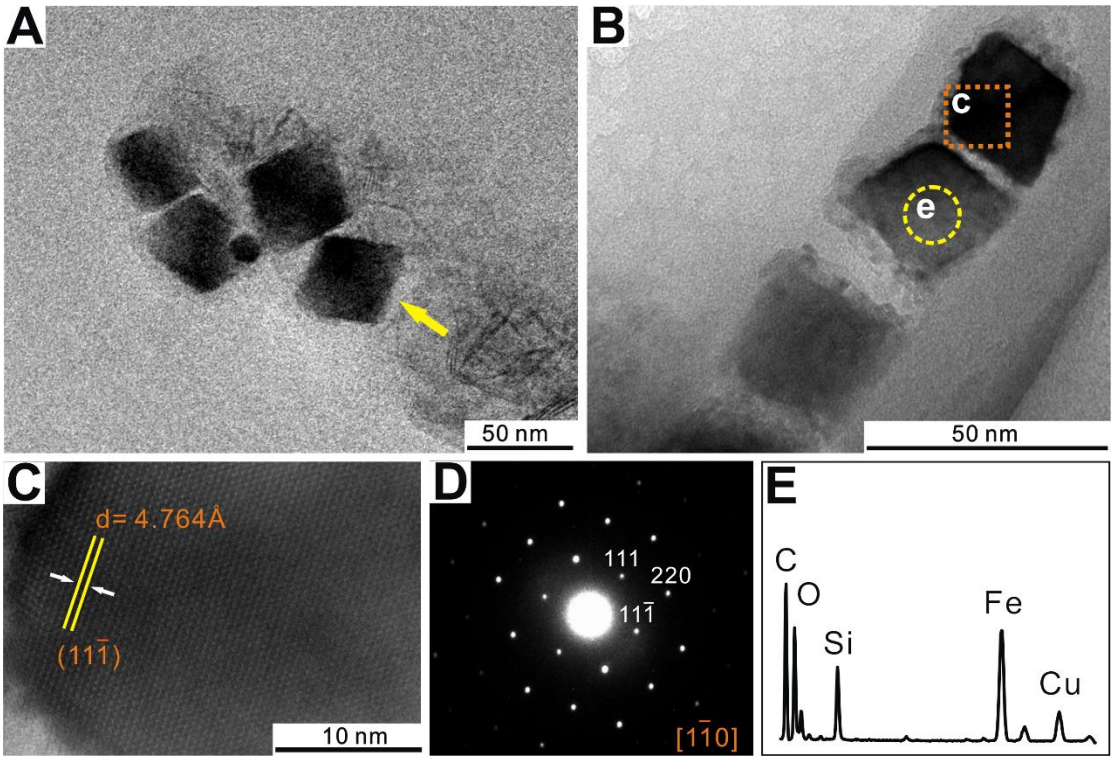

图 1. 磁小体化石的 TEM 照片。A-B: 从西太平洋锰结核中提取的立方八面体磁小体 TEM 图像（中的黄色箭头表示磁化石链，橙色方框和黄色圆圈分别表示高分辨率 TEM 图像和 EDS 分析位置）。C-E：高分辨率图像、电子衍射和 EDS 结果（Cu 峰来源于 TEM 网，C 峰来源于碳膜，Si 信号来源于被分析粒子附近的硅质碎屑）。

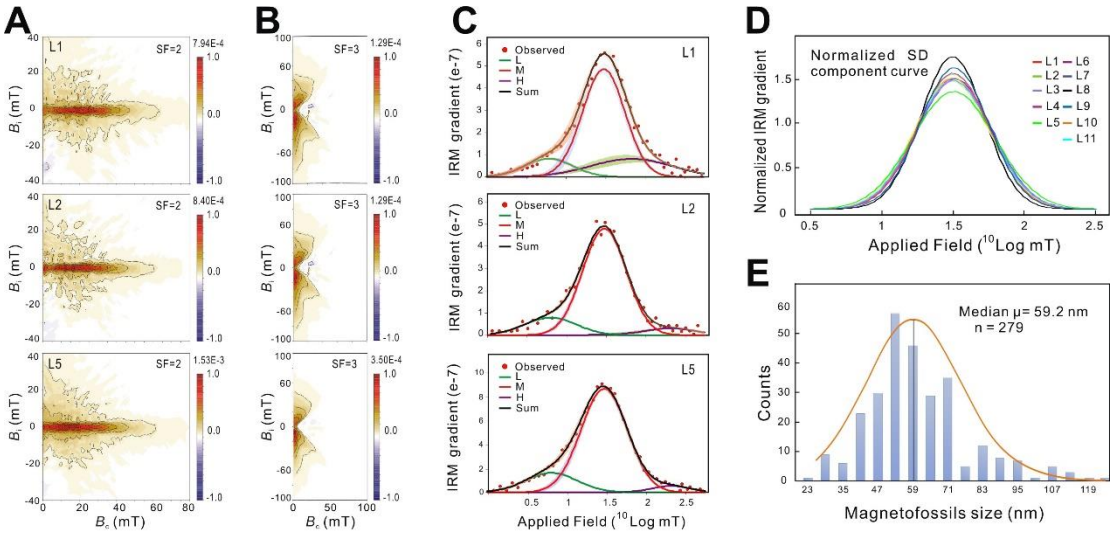

图 2. 锰结核切片代表性的磁学数据。A: 具有代表性的 FORC 图，图中均包含沿矫顽力轴方向的独特的中心脊，这些脊表示非相互作用的单轴 SD 颗粒。B：具有代表性的 tFORC 图，它们都沿着双轴有两个“翅膀”，表示旋涡或多畴状态（Roberts et al., 2017; Zhao et al., 2017） （即低矫

顽力 IRM 分量）。C：FORC 测量标本的 IRM 成分分析。红点表示定义 IRM 采集曲线梯度的数据点，低（L，绿色）中（M，红色）和高矫顽力（H，紫色）表示。M 分量表示磁小体化石，每个组分的着色底纹表示各自的 95%置信范围。D 不同样品切片的归一化中间矫顽力曲线。E：磁小体化石粒径柱状分布图。

参考文献：

Jiang Xiaodong; Zhao Xiang; Chou Yumin; Liu Qingsong*; Roberts P Andrew; Ren Jiangbo; Sun Xiaoming; Li Jinhua; Tang Xu; Zhao Xiangyu; Wang Chun-Chieh; Characterization and quantification of magnetofossils within abyssal manganese nodules from the Western Pacific Ocean and implications for nodule formation, Geochemistry, Geophysics, Geosystems, 2020, e2019GC008811.*

Jiang Xiaodong; Gong Junli; Ren Jiangbo; Liu Qingsong; Zhang Jiang; Chou Yumin; An interdependent relationship between microbial ecosystems and ferromanganese nodules from the Western Pacific Ocean, Sedimentary Geology, 2020, 398, 105588.*

文献导读

1. 在河流中以絮凝和悬浮的河床物质运输的泥质研究

翻译人：仲义 zhongy@sustech.edu.cn

Michael. P. Lamb, Jan de Leeuw, Woodward W. Fischer., et al., ***Mud in rivers transported as flocculated and suspended bed material*** *[J]. Nature Geoscience, 2020, 13 (8), 566-570.* https://doi.org/10.1038/s41561-020-0611-4.

摘要：粉砂和黏土颗粒或泥质沉积物为主河流搬运物质组成地球表面主要成分，并控制着地球表面沉积物及有机碳的输送。相比于砂质通量变化，泥质通量变化很难被预测。然而，理解泥质河流沉积物的动力学特征对于全球碳循环、海岸带景观对海平面的恢复效应、河流恢复及地球和火星上的河漫滩形态动力学都有重要意义。长期以来悬砂输运的力学理论一直存在，但是对于河流中的泥质沉积物常常被认为是构成冲刷载荷的主要因素，由于泥质沉积物沉降速度过慢，以致于其与河床之间没有相互作用，只能依托于上游的供应，并且不可能作为当地水文动力学来预测。为了验证这个假说，作者从 8 条河流的文献数据中汇编了泥质浓度剖面含量，利用反演技术来确定悬浮泥的沉降速率。作者发现河流中泥质沉积物主要以絮凝体存在，沉降速度几乎恒定，与颗粒大小无关，约为 0.34 mm/s，比单个颗粒沉降速度快 100 倍。研究表明，絮凝泥是悬浮床质荷载的一部分，并非为冲刷荷载，因此可以用床质夹带理论进行物理描述。

ABSTRACT: Riverine transport of silt and clay particles—or mud—builds continental landscapes and dominates the fluxes of sediment and organic carbon across Earth’s surface. Compared with fluxes of sand-sized grains, mud fluxes are difficult to predict. Yet, understanding the fate of muddy river sediment is fundamental to the global carbon cycle, coastal landscape resilience to sea-level rise, river restoration and river–floodplain morphodynamics on Earth and Mars. Mechanistic theories exist for suspended sand transport, but mud in rivers is often thought to constitute washload—

sediment with settling velocities so slow that it does not interact with the bed, such that it depends only on upstream supply and is impossible to predict from local hydraulics. To test this hypothesis, we compiled sediment concentration profiles from the literature from eight rivers and used an inversion technique to determine settling rates of suspended mud. We found that mud in rivers is largely flocculated in aggregates that have near-constant settling velocities, independent of grain size, of approximately 0.34 mm s-1, which is 100-fold faster than rates for individual particles. Our findings indicate that flocculated mud is part of suspended bed-material load, not washload, and thus can be physically described by bed-material entrainment theory.

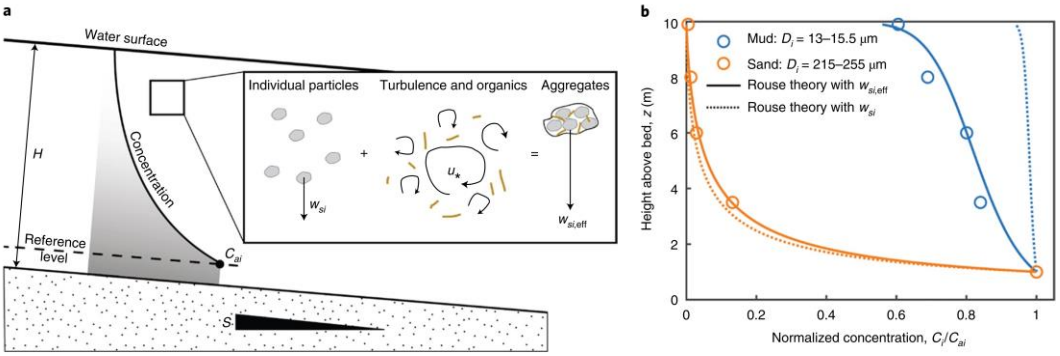

Figure 1. Sediment suspension profiles. a, Schematic cross-section of H and bed slope S showing a concentration profile governed by Wsi and u*. Flocculation increases w si,eff, resulting in a greater concentration gradient with depth. b, Example grain-size-specific vertical concentration profiles from the Ganges River38 showing that sand follows Rouse theory (equation (1)), whereas the mud fraction deviates substantially from theory when using Wsi. The best-fit Rouse number was used to find W si,eff.

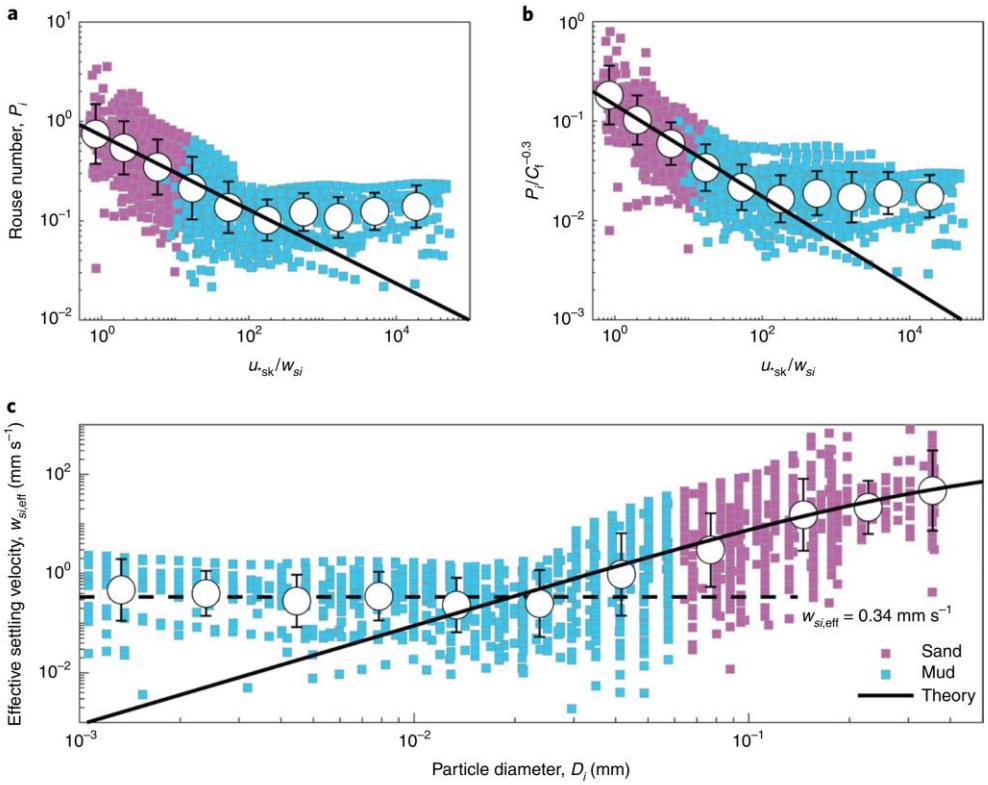

Figure 2. Mud transport data compared to theory. a, Best-fit Rouse parameters, Pi, from suspension profiles versus u*sk, normalized by wsi, showing systematic deviation of the mud fraction from a one-parameter model for sand20 with βi ¼ 3:4 - uw*sk si0:63(Methods). Each square represents a grain-size specific concentration profile, and larger circles are binned geometric means ± 1 s.d. (error bars). b, Same as a but Rouse parameters were normalized to account for the secondary dependence of βi on Cf in the two-parameter model for sand20 with βi ¼ 16:82 - uw*sk si 0:54C0 f :3(Methods). c, Effective settling velocities derived from concentration profiles as a function of particle diameter, showing that the mud fraction systematically deviates from theory39(black line) for settling of individual particles (Methods). The legend in c applies to all panels.

2. 从中大西洋洋脊获得的循环弧地幔

翻译人：冯婉仪 fengwy@sustech.edu.cn

Urann B M, Dick H J B, Parnell-Turner R et al. ***Recycled arc mantle recovered from the Mid-Atlantic Ridge****[J]. Nature communications, 2020, 11: 3887.*

https://doi.org/10.1038/s41467-020-17604-8

摘要：板块构造理论和地幔动力学需要地幔循环存在于整个地球历史中，但仍然难以找到地幔再循环过程的直接地球化学证据。在这里，我们展示了从 16° 30′ N 附近的中大西洋洋脊挖出了循环的俯冲带地幔楔橄榄岩的证据。橄榄岩的微量元素特征不支持与典型的洋中脊构造背景相关的分离无水熔融作用。相反，这些样品的成因最合理的解释是它们经历了含水交代熔融，而且熔融反应的改变导致单斜辉石在高程度熔融的条件下没有被消耗完，并且保留在残余体中。根据沿着轴向洋脊深度的变化，这种有浮力的难熔弧地幔在深部可能被地幔中密度更大的且可能富含石榴石的岩性所补偿。我们的研究结果表明，高度难熔的弧地幔残余体被夹带在上地幔中，而且它们可能至少占上地幔体积的 60%。这些高度难熔的地幔域对地幔熔融的贡献不大，因此，仅依赖于玄武岩成分反演地幔成分可能难以发现它们的存在。

ABSTRACT: Plate tectonics and mantle dynamics necessitate mantle recycling throughout Earth’ s history, yet direct geochemical evidence for mantle reprocessing remains elusive. Here we present evidence of recycled supra-subduction zone mantle wedge peridotite dredged from the Mid-Atlantic Ridge near 16° 30′ N. Peridotite trace-element characteristics are inconsistent with fractional anhydrous melting typically associated with a mid-ocean ridge setting. Instead, the samples are best explained by hydrous flux melting which changed the melting reactions such that clinopyroxene was not exhausted at high degrees of melting and was retained in the residuum. Based on along-axis ridge depth variations, this buoyant refractory arc mantle is likely

compensated at depth by denser, likely garnet-rich, lithologies within the mantle column. Our results suggest that highly refractory arc mantle relicts are entrained in the upper mantle and may constitute >60% of the upper mantle by volume. These highly refractory mantle domains, which contribute little to mantle melting, are under-represented in compilations of mantle composition that rely on inverted basalt compositions alone.

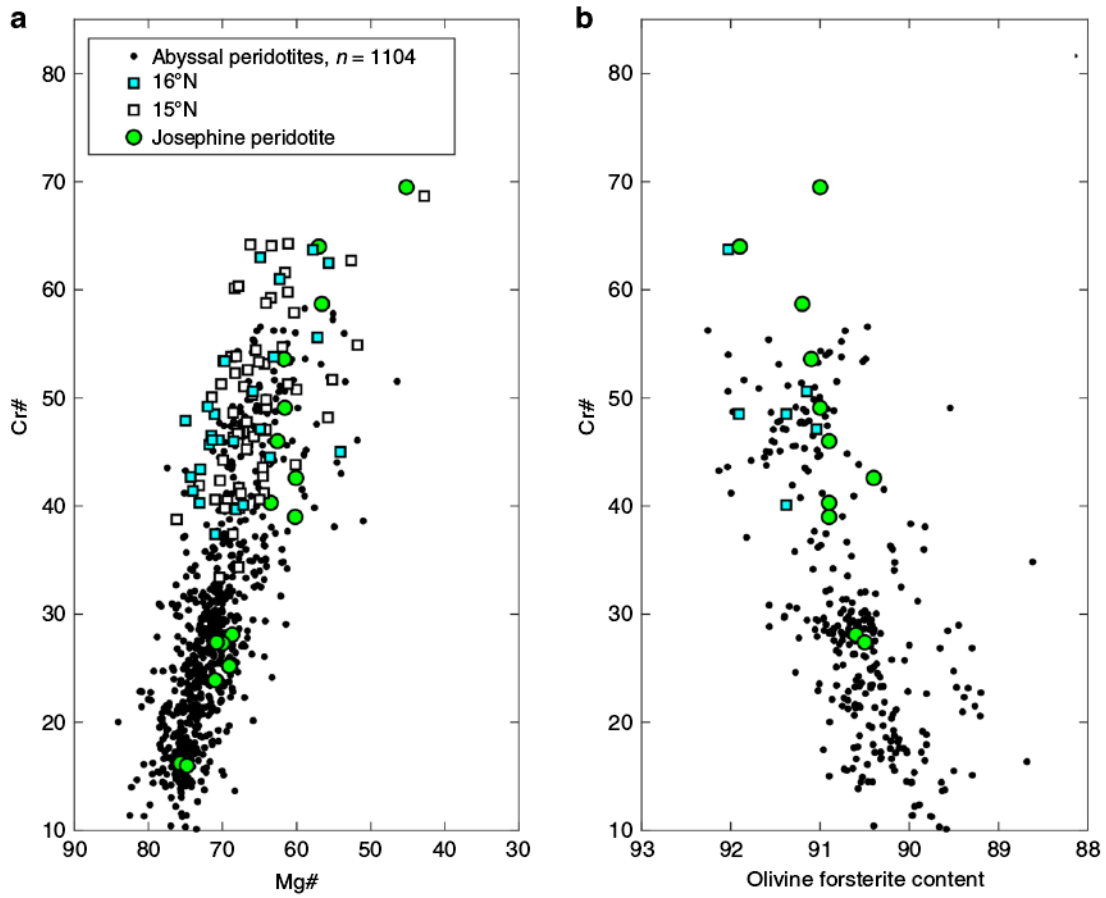

Figure 1. Chromian spinel and olivine compositions of 14–16°N peridotites compared to abyssal peridotites. a Cr# after Dick et al.[40]. b Spinel Cr# plotted against coexisting olivine forsterite content. Josephine peridotite, a well-known SSZ locality, plotted for comparison with data from Le Roux et al. [39]. Abyssal peridotite data from the compilation of Warren[42]. Not all spinel–olivine pairs were analyzed due to alteration. Analytical uncertainties smaller than symbols.

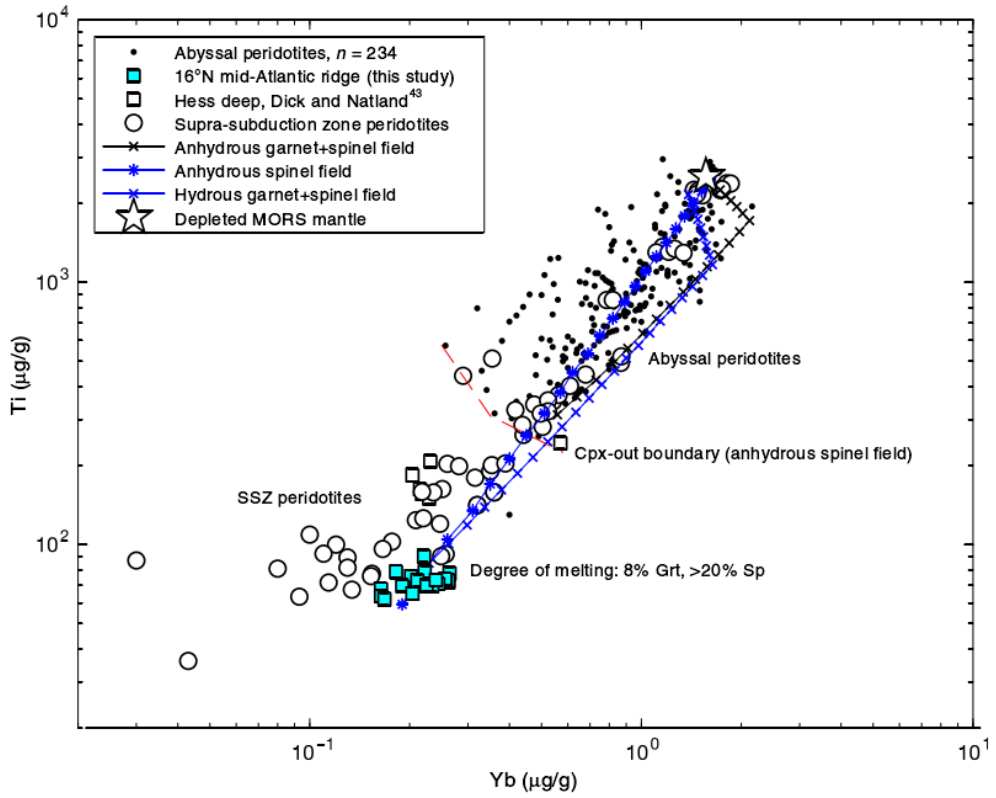

Figure 2. Fractional melting model of incompatible elements titanium and ytterbium in clinopyroxene. Anhydrous melting alone cannot replicate the ultra-refractory Cpx compositions before Cpx is exhausted, whether one considers spinel field or garnet followed by spinel field (black ticked line) melting. However, changes in melting modes and partition coefficients in a hydrous melting environment permit extreme depletions in Ti, matching observations (blue lines). Cyan squares represent each individual measurement from 16°N Cpx (Supplementary Data 2). Red dashed line is approximate spinel-field Cpx-out boundary based on modeled anhydrous melting of DMM spinel bearing peridotite. Model details, including melting modes and partition coefficients, can be found in the Methods section and Supplementary Data 5. SSZ peridotites are thought to have undergone extreme degrees of melting in a mantle wedge setting, often resulting in the exhaustion of Cpx; SSZ Cpx Ti and Yb abundances are very similar to those observed in 16° N Cpx. Abyssal peridotite data from the literature as compiled by Warren[42]. SSZ peridotite data from the literature[36–39].

3. 白垩纪末期德干高原火山活动和全地幔对流期间的低地磁场强度

翻译人：李园洁 liyj3@sustech.edu.cn

Radhakrishna T, Mohamed A R, Venkateshwarlu M, et al. Low geomagnetic field strength during End-Cretaceous Deccan volcanism and whole mantle convection[J]. Scientific reports, 2020, 10(1): 1-6. https://doi.org/10.1038/s41598-020-67245-6

摘要：由于缺乏可靠的地质历史时期的地磁场实验数据，目前地磁偶极子场的长期变化的认识仍处于初级阶段。本文，我们第一次给出来自地球上白垩纪期间最大的火成岩省的古地磁数据，~65-66Ma 德干高原玄武岩 1250m 厚的到基底的地层剖面，来自 Koyna Deep Scientifc Drilling Project 中印度西高止山的一个钻孔。对结果的分析发现：(i)整个白垩纪期间末期德干高原喷发期间地磁场磁偶极矩最低；(ii) 白垩纪正极性超时开始或结束时的磁偶极矩比中间的更低，但这种差异不能解释为更短的极性时间，因为没有足够的时间形成可识别的变化；(iii) 不存在磁偶极矩和倒转频率的负相关关系；(iv) 核-幔边界热流与低磁偶极矩之间的因果关系可能控制地球表面上大火成岩省的形成的主要因素。

ABSTRACT：Knowledge about long-term variation of the geomagnetic dipole field remains in its nascent stage because of the paucity of reliable experimental data over geological periods. Here, we present the first robust experimental data from the largest Cretaceous flood basalt province on Earth, the ~65-66Ma Deccan basalt within a thick (1250m) unbiased stratigraphic section down to the basement, recovered from a drill hole of the Koyna Deep Scientific Drilling Project in the Western Ghats, India. Critical analysis of the result along with similar results of the Cretaceous age find that (i) the dipole moment during the end Cretaceous Deccan eruption is the lowest in whole of Cretaceous (ii) dipole moment at the onset/termination of the Cretaceous Normal Superchron is apparently lower relative to that in midsuperchron, however, such differences cannot be deciphered in shorter polarities probably because of insufficient time to develop recognizable variations (iii) inverse relation between dipole moment and reversal rate is lacking and (iv) a cause and effect relation between core-mantle

boundary heat flux and low dipole moment that appears to be the principle governing factor in forming the Large Igneous Provinces on the surface of earth.

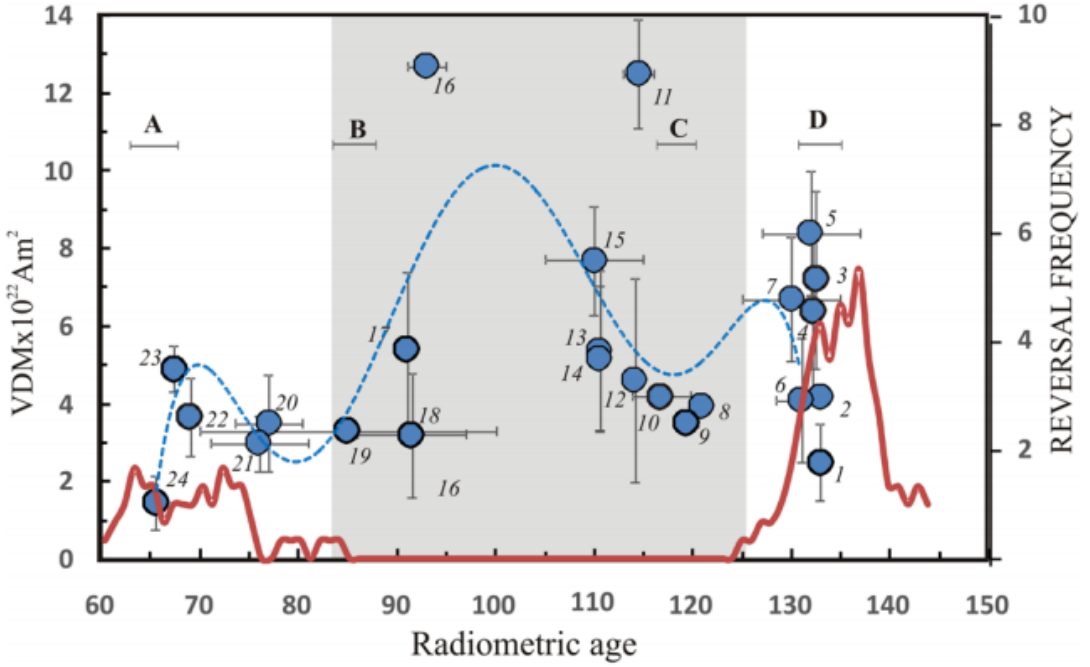

Figure 1. Distribution of VDM data during the Cretaceous period. The data set is as listed in table S-T2. Note a polynomial trend showing high dipole moment with low values on either end of the CNS. The numbers next to the data points are linked to the serial numbers in table S-T2. Also shown are the timing of mantle plumes of the Cretaceous responsible for the major large igneous provinces marked as A, B, C and D: A denotes the Reunion related Deccan food basalt (and near synchronous ~62 Ma North Atlantic Tertiary Volcanic Province), B denotes the Marion plume related Madagascan igneous province (and near synchronous ~ 90 Ma Ontong Java plateau), C denotes the Kerguelen plume related Rajmahal volcanism and D denotes the Tristan da Cunha plume related Parana basalts. The ages of these LIPs are shown with error bars. It can be seen the low dipole moments correspond to the mantle plumes/LIPs in age. Area coverage of LIPs in each age bracket (A: >3; B: <3.5; C: ~2 and D: ~1.5 in million km^2) may indicate a measure of their magnitudes. Polarity reversal frequency with 3 Ma running average from the 2012 GPTS is shown in red line. The grey shade demarcates the CNS.

4. 关于尘埃冰记录剩磁的实验证据

翻译人：柳加波 liujb@sustech.edu.cn

Grossman Y, Aharonson O, Shaar R, et al. ***Experimental determination of remanent magnetism of dusty ice deposits[J]****. Earth and Planetary Science Letters, 2020, 545: 116408.* *https://doi.org/10.1016/j.epsl.2020.116408*

摘要：类似于沉积岩，冰和粉尘的混合物在不断积累和沉积的过程中也可能会记录剩磁。本文，我们认为粉尘在空气中沉降并具有方向选择性，从而在附着过程中能够记录外在磁场。我们用一个简单的模型对含有磁性包裹体的冰粒的沉降和重新定向进行了研究。该模型包括磁扭矩、空气动力和重力，从而研究控制过程中的参数空间。对介于 10's 到 100's μT 范围内的磁场，我们发现包含较小的磁性颗粒的作为核，并且尺寸低于 100 μm 的冰粒，能够产生于外加磁场一直的沉积剩磁方向，但是磁矩和外加磁场强度不一致。对于 100 μm 以内的冰粒，磁矩随外加场强度增加。为了通过实验证明这种作用，我们进行了一系列实验室沉积模拟，然后测量样品的磁矩。我们发现，在理想化的实验室条件下，尘埃冰会在施加磁场的方向上磁化，并且排列随强度的增加而增加。在特定的条件下，磁化强度会随着场强在 10–200 μT 范围内的增加而迅速增加，并在此之上达到最大值。对于具有粉尘/冰比为 5×10^{-3} 的混合物，我们获得了最大磁化值范围为 $1.6\times10-5$ – $3\times10-3\,\mathrm{A\,m^2/kg}$，具体取决于粒径分布。我们认为，冰中的磁性粒子浓度决定了剩磁的水平，并得出结论，在各种环境下天然冰沉积物的剩余磁化强度是可以测量的（如果不受沉积后、风或其他因素的影响），因此可能提供关于地球和其他行星的新古磁记录。

ABSTRACT: Accumulations of ice and dust mixtures may acquire magnetization during deposition in a manner analogous to sedimentary rocks. Here, we consider the process of particles descending through an atmosphere and depositing in a preferential orientation that serves to record the ambient magnetic field during emplacement. We

use a simple model for the settling and reorientation of ice particles with magnetic inclusions that includes magnetic torque, aerodynamic forces and gravity, to investigate the parameter space governing the process. For fields in the range of 10's – 100's μT we find that ice particles of sizes up to ~100 μm which contain smaller magnetic grains as nuclei will produce a deposit indeed magnetized in the direction aligned with the applied field, but with a moment that is independent of the field strength. For particles in the 100's μm range, the magnetic moment increases with the field strength. To demonstrate the effect experimentally, we performed a suite of laboratory deposition simulations followed by measurements of the magnetic moment of the samples. We show that in the idealized laboratory conditions dusty ice magnetizes in the direction of the applied field, with the alignment increasing with its intensity. For the chosen conditions, the magnetization increases rapidly with field intensity in the range 10 – 200 μT, and approaches a maximal value above that. For a mixture with dust/ice ratio of 5×10^{-3} we obtained maximal magnetization values in the range $1.6\times10-5$ – $3\times10-3$ A m^2/kg, depending on the distribution of particle sizes. We show that magnetic particle concentration in the ice determines the level of magnetic remanence, and conclude that the remanent magnetization of natural ice deposit in various settings may be measurable (if unobscured by post-depositional, wind, or other effects) and thus could provide a new paleomagnetic record on Earth and other planetary objects.

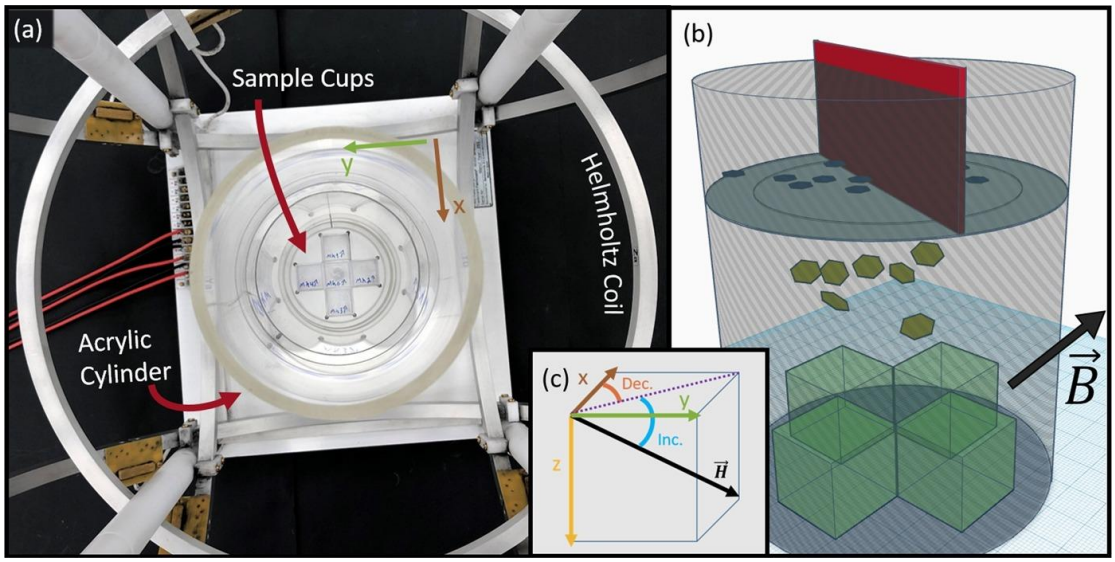

Fig 1: An overview of the experimental setup in plan (a) and oblique (b) views. An ice and magnetite particles mixture is placed on a sieve (gray disk) in the upper portion of a 0.2 m tall acrylic cylinder. With the help of a rotating blade (red rectangle), the mixture is gradually sieved through a mesh, settling into five 6 cm^3 sample cups (green cubes) at the base. During descent, a uniform magnetic field B→ acts to reorient the particles. (c) The directional convention of the applied field.

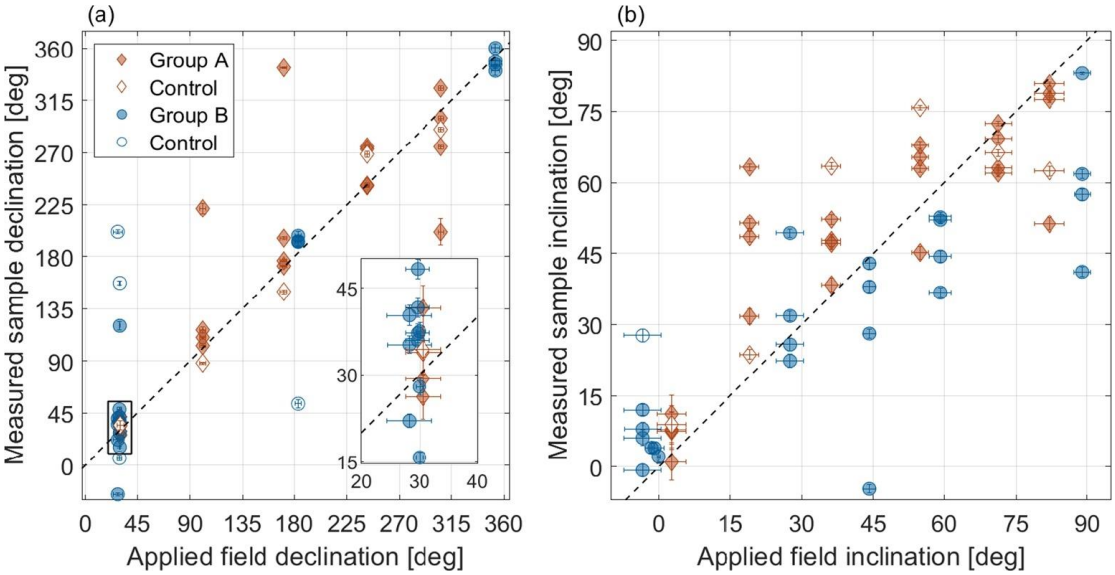

Fig 2: Measured magnetization declination (a) and inclination (b) of dusty ice vs. declination and inclination, respectively, of magnetic field applied during deposition. Orange diamonds and blue circles represent samples of group A (particle size 125<D<355μm) and B (D<2000μm), respectively. Note that

the applied fields are plotted as the measured values, that may differ slightly from those in Table 1. Control samples (empty markers) are plotted along with the property of the field that was activated after their deposition (during the deposition of the corresponding variable samples of its batch).

5. 菲律宾巴拉望-民都洛地块锆石 U-Pb 年代学和 Hf 同位素特征---对南海构造演化和物源的指示

翻译人：刘伟 inewway@163.com

Yan Y , Yao D , Tian Z , et al. Zircon U-Pb Chronology and Hf Isotope From the Palawan-Mindoro Block, Philippines: Implication to Provenance and Tectonic Evolution of the South China Sea[J]. Tectonics, 2018, 37(3-4):1063-1076.

https://doi.org/10.1002/2017TC004942

摘要：东南亚大陆边缘由中生代以安第斯型为主的活动边缘演化为晚白垩世以来的西太平洋型活动边缘。随着南海的扩张，巴拉望-民都洛地块从亚洲大陆漂移而来，其新生代地层为解析东南亚边缘的构造演化提供了很好的视角。本文对菲律宾巴拉望-民都洛地块新生代沉积岩碎屑锆石颗粒进行了 U-Pb 年龄和 Hf 同位素分析，以研究南海的物源和构造演化。巴拉望-民都洛地块始新世中新世沉积岩锆石颗粒年龄范围较广，从 60～2700 Ma，主要有 80～120 Ma、160～180 Ma、1600～2100 Ma、2200～2700 Ma 四个年龄组份。民都洛岛样品锆石颗粒的 Hf(t)在-39 ～ +13.7 之间，在古近系和新近系层中记录到相似的 Hf 同位素组成。巴拉望-民都洛地块始新世样品的锆石 U-Pb 年龄和 Hf 同位素特征与台湾地区的样品相似，说明巴拉望-民都洛地块在晚白垩世始新世位于华南边缘。台湾与巴拉望-民都洛地块中新世样品中锆石 U-Pb 年龄组成的差异反映了当时巴拉望-民都洛地块的南移和南海海底扩张。

ABSTRACT: The continental margin of Southeast Asia evolved from a dominantly Andean-type active margin during Mesozoic to a Western Pacific-type since Late Cretaceous. With the spreading of the South China Sea, the Palawan-Mindoro Block drifted from mainland Asia and the Cenozoic strata provide an excellent window to gain insights into the tectonic evolution of the margin of Southeast Asia. Here we present U-Pb age and Hf isotopic data on detrital zircon grains from Cenozoic sedimentary rocks

in the Palawan-Mindoro Block, Philippines, to evaluate the provenance and tectonic evolution of the South China Sea. Zircon grains in Eocene-Miocene sedimentary rocks from the Palawan-Mindoro Block show a wide range in age from 60 to 2700 Ma, with four major age groups of 80–120 Ma, 160–180 Ma, 1600–2100 Ma, and 2200–2700 Ma. The εHf(t) of the zircon grains of the samples from Mindoro Island range from −39 to +13.7, and similar Hf isotopic composition is recorded in Paleogene and Neogene strata. Zircon U-Pb ages and Hf isotopic data of the Eocene samples from the Palawan-Mindoro Block show a similar pattern with those from Taiwan, which suggests that the Palawan-Mindoro Block was attached to the margin of South China during Late Cretaceous-Eocene times. The difference of zircon U-Pb age composition in the Miocene samples between the Palawan-Mindoro Block and Taiwan reflects southward drifting of the Palawan-Mindoro Block and seafloor spreading of the South China Sea at that time.

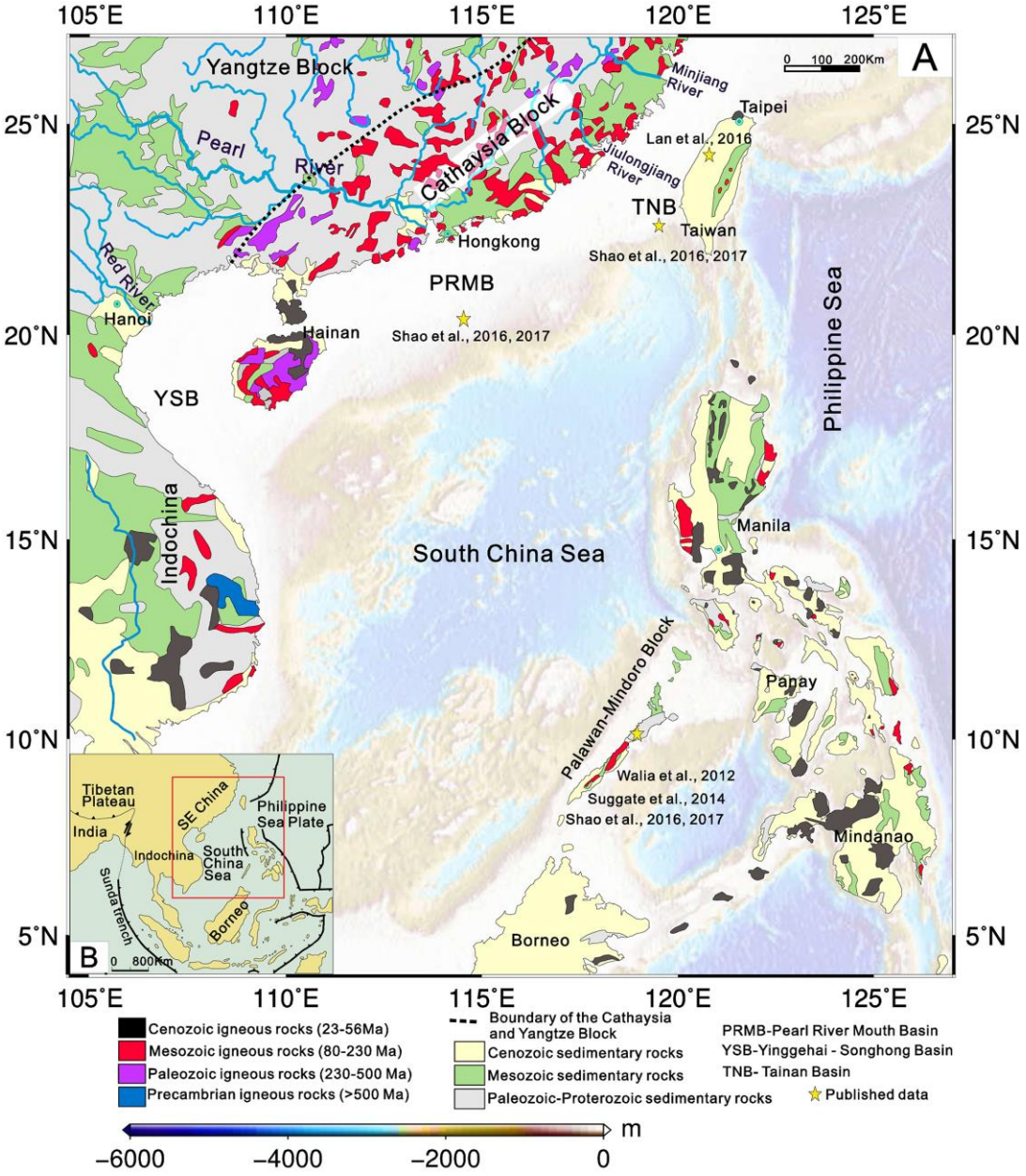

Figure 1. A: Geological map of Southeast Asia, showing the spatial-temporal distribution of crystalline basement and stratigraphic units. B: Simplified tectonic map of East Asia and the environs of the South China Sea (Ma, 2001).

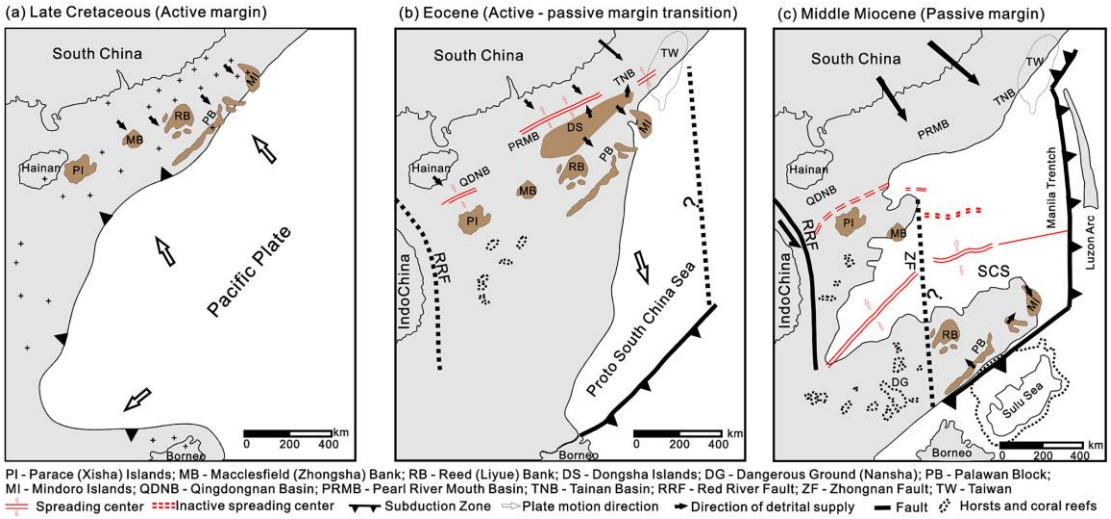

Figure 2. Paleogeographic reconstruction (after Hall & Breitfeld, 2017; Li et al., 2014) and provenance evolution of the margin of Southeast Asia from (a) Late Cretaceous to (b) Eocene and (c) Miocene.

6. 胡安德富卡洋中脊“奋进”段的热液烟囱分布

翻译人：曹伟 11930854@QQ.com

Clague D A , Martin J F , Paduan J B , et al. Hydrothermal Chimney Distribution on the Endeavour Segment, Juan de Fuca Ridge[J]. Geochemistry, Geophysics, Geosystems, 2020, 21.

https://doi.org/10.1029/2020GC008917

摘要：胡安德富卡洋中脊的“奋进”段以其丰富的热液喷口和烟囱而闻名。自主潜航器收集到的 1 米精度多波束测绘数据显示，距该航段中心 14 公里范围内共有 572 个烟囱，其中只有 47 个已知活跃烟囱并被命名。热液沉积被限制在地震映射的轴向岩浆透镜体上方的轴向地堑以及地堑近缘。在过去的 4300 年里，该段稀疏的喷发活动并没有像在岩浆作用更强的洋山脊上那样掩埋不活跃的海底烟囱。

ABSTRACT: The Endeavour Segment of the Juan de Fuca Ridge is well known for its abundance of hydrothermal vents and chimneys. One-meter scale multibeam mapping data collected by an autonomous undersea vehicle revealed 572 chimneys along the central 14 km of the segment, although only 47 are named and known to be active. Hydrothermal deposits are restricted to the axial graben and the near-rims of the graben above a seismically mapped axial magma lens. The sparse eruptive activity on the segment during the last 4,300 years has not buried inactive chimneys, as occurs at more magmatically robust mid-ocean ridges.

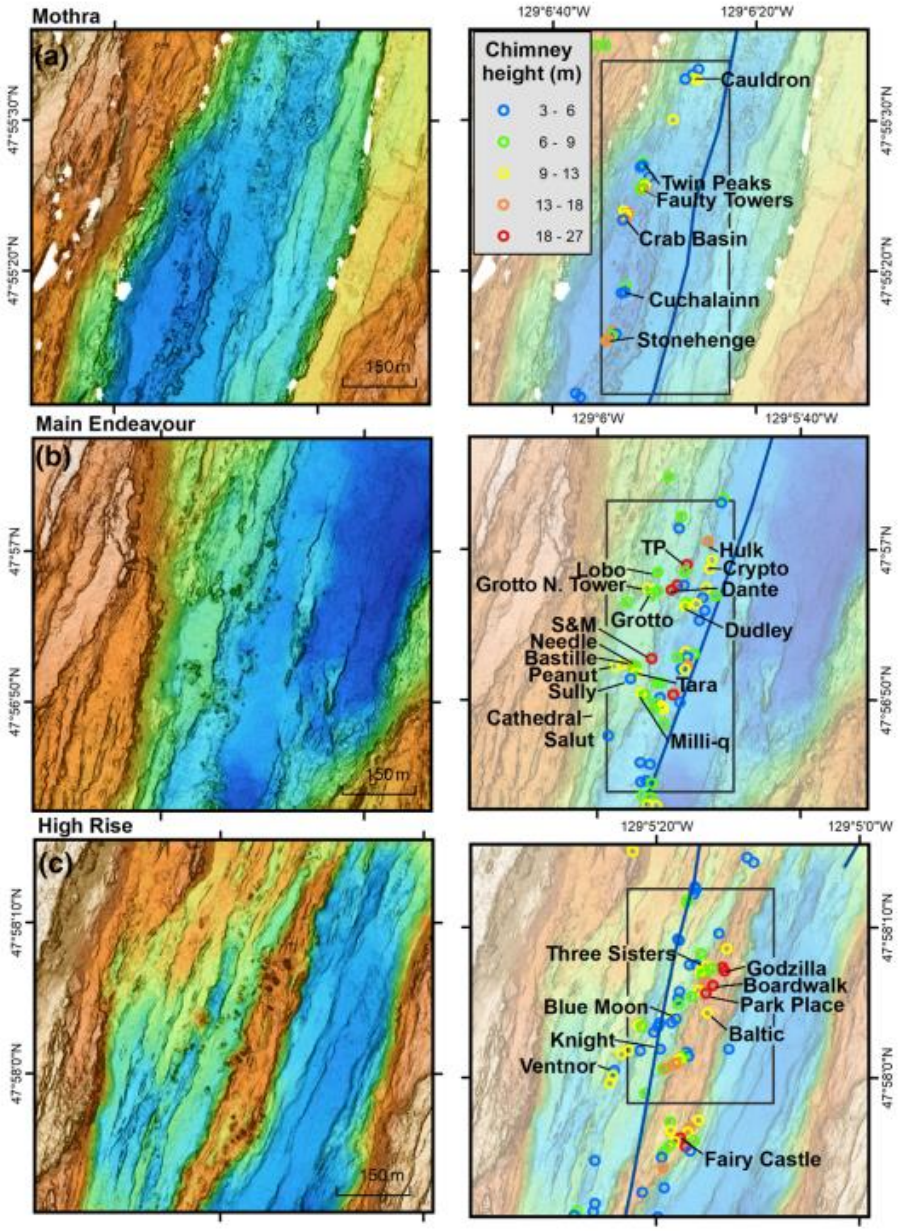

Figure 1. AUV bathymetry maps of the (a) Mothra (b) Main Endeavour, and (c) High Rise active hydrothermal vent fields on Endeavour subsegment AV2a (Le Saout et al., 2019). The right panel shows faded bathymetry with circles marking chimney locations identified from the AUV data; symbol colors indicate chimney height measured from the AUV data. Black boxes outline the extents of the previously named active vent fields (Glickson et al., 2007). Vent names from Robigou et al. (1993), Delaney et al. (1992), and Glickson et al. (2007). All maps are gridded at 1 m and plotted at a scale of 1:10,000. Color scale has been histogram equalized for each map.

7. 从利用一种同位素模型解释中国石笋氧同位素记录

翻译人：杨会会 11849590@mail.sustech.edu.cn

Hu J, Emile G J, Tabor C et al. Deciphering oxygen isotope records from Chinese speleothems with an isotope-enabled climate model[J].Paleoceanography and Paleoclimatology, 2019, 34, 12:2098–2112

https://doi.org/10.1029/2019PA003741

摘要：石笋 δ18O 记录被广泛应用于重建过去水文气候变化，尤其是在亚洲。然而，这一指标的解译还在讨论中。虽然这个指标最初被解释为亚洲季风的区域降雨量，但其他研究将其解释为上游季风降雨或大气环流的变化。为了更好地理解不同时间尺度下石笋中保存的信号，本研究采用了最先进的同位素气候模型来量化中国降水氧同位素（$\delta^{18}OP$）的组成。结果显示中国石笋 $\delta^{18}O$ 在轨道尺度上主要记录了亚洲季风环流的纬向迁移，以及东亚雨带早期的北向迁移。在年际尺度上，中国石笋 $\delta^{18}O$ 也通过水汽源地的变化，与季风环流的强度有关：来自遥远水汽源地区的水汽输送增强使 $\delta^{18}O$ 更加偏负，特别是在夏末和初秋。我们的研究结果对中国洞穴的水文气候解释有一定的指导意义，并表明这种解释与时间尺度有关。

ABSTRACT: Speleothem $\delta^{18}O$ is widely used to reconstruct past hydroclimate variability, particularly over Asia. However, the interpretation of this proxy is still in debate. While this proxy is originally interpreted as regional rainfall amount of the Asian monsoon, other studies have interpreted it as upstream monsoon rainfall or atmospheric circulation changes. To better understand the signal preserved in speleothems over various time scales, this study employs a state-of-the-art isotope-enabled climate model to quantify contributions to the oxygen isotope composition of precipitation ($\delta^{18}O_P$) over China. Results suggest that orbital-scale speleothem $\delta^{18}O$ variations at Chinese sites mainly record the meridional migration of the Asian

monsoon circulation, accompanied by an early northward movement of the East Asian rain belt. At interannual scales, Chinese speleothem $\delta^{18}O$ is also tied to the intensity of monsoonal circulation, via a change in moisture source locations: Enhanced moisture delivery from remote source regions leads to more negative $\delta^{18}O_P$, particularly in late summer and early autumn. Our results have implications for the hydroclimatic interpretation of speleothem $\delta^{18}O$ from Chinese caves and suggest that this interpretation is time scale dependent.

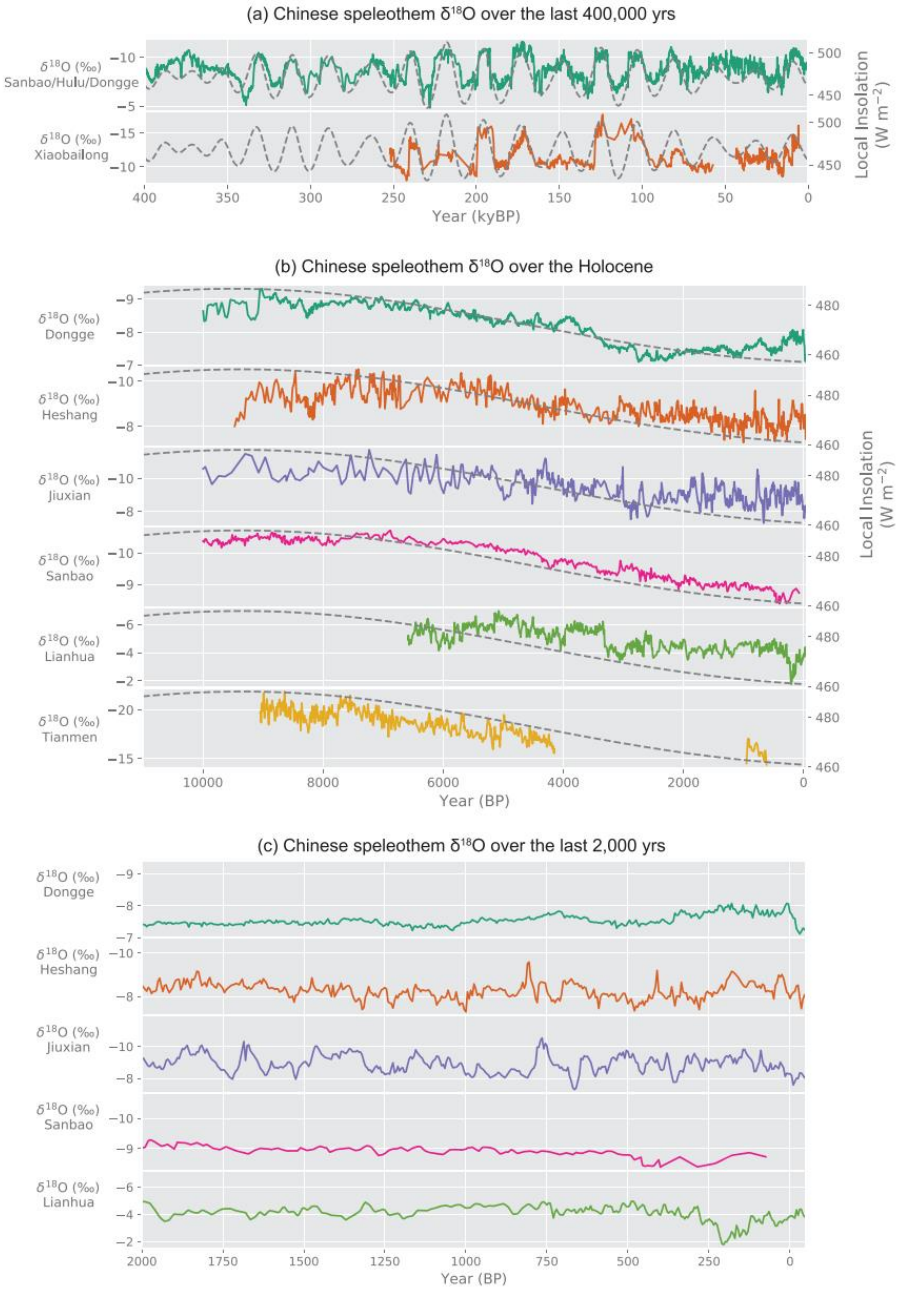

Figure 1. (a) Chinese speleothem $\delta^{18}O$ over the last 400,000 years (colored solid lines) with their local

summer JJA insolation (gray dashed lines). $\delta^{18}O$ in the first panel is a composite of three Chinese records (Sanbao, Hulu, and Dongge Caves) in Cheng et al. (2016). (b) Chinese speleothem $\delta^{18}O$ over the Holocene with their local summer insolation. (c) Chinese speleothem $\delta^{18}O$ over the last 2,000 years.

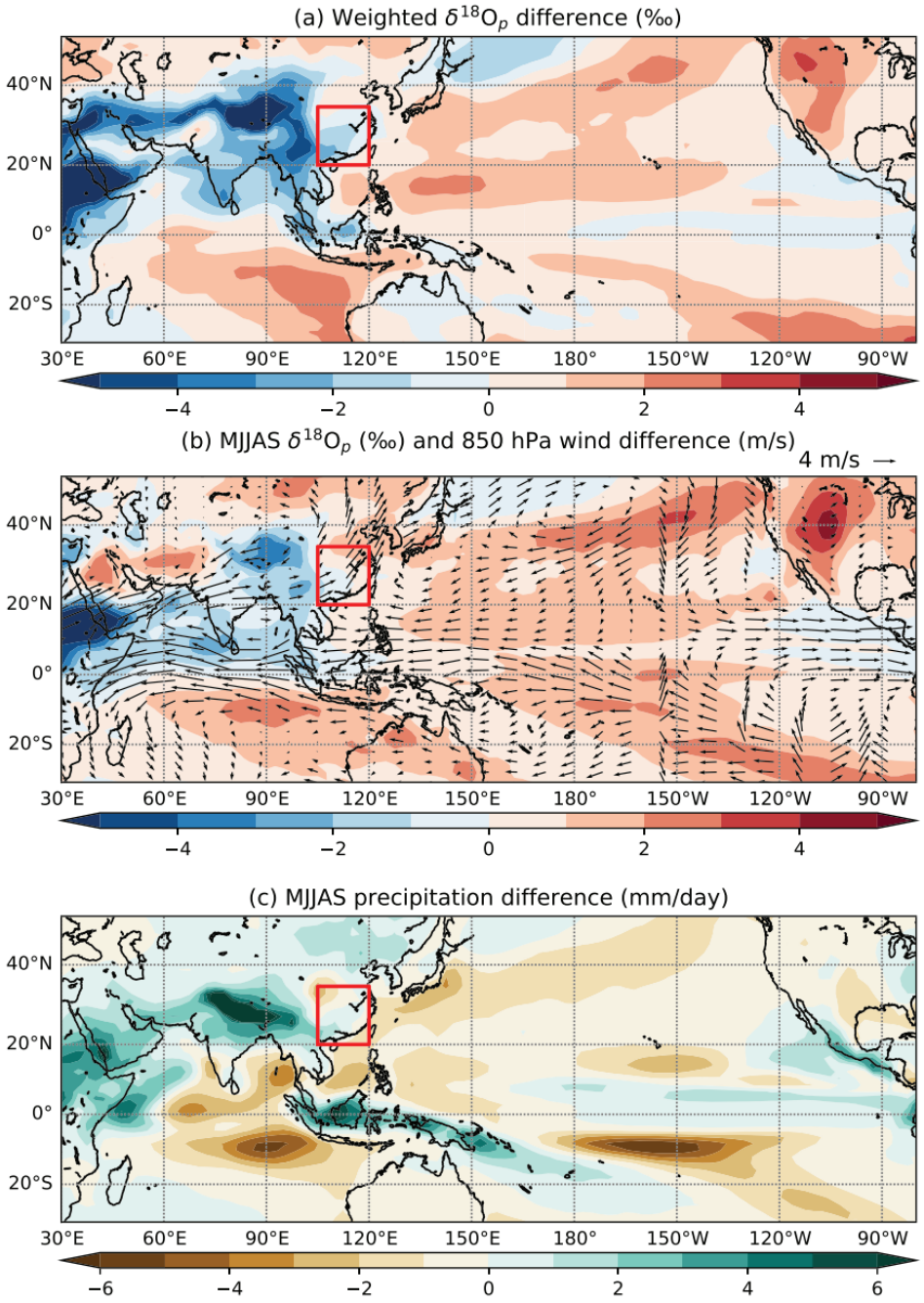

Figure 2. Difference between precession minimum (maximum of the Northern Hemisphere summer insolation) and maximum (minimum of the Northern Hemisphere summer insolation). (a) Weighted $\delta^{18}O_P$ difference, (b) MJJAS $\delta^{18}O_P$ and 850-hPa wind difference. (c) MJJAS precipitation difference. The red box is the defined region of East China, and its mean precipitation and $\delta^{18}O_P$ is in Figures 5a and 5b.

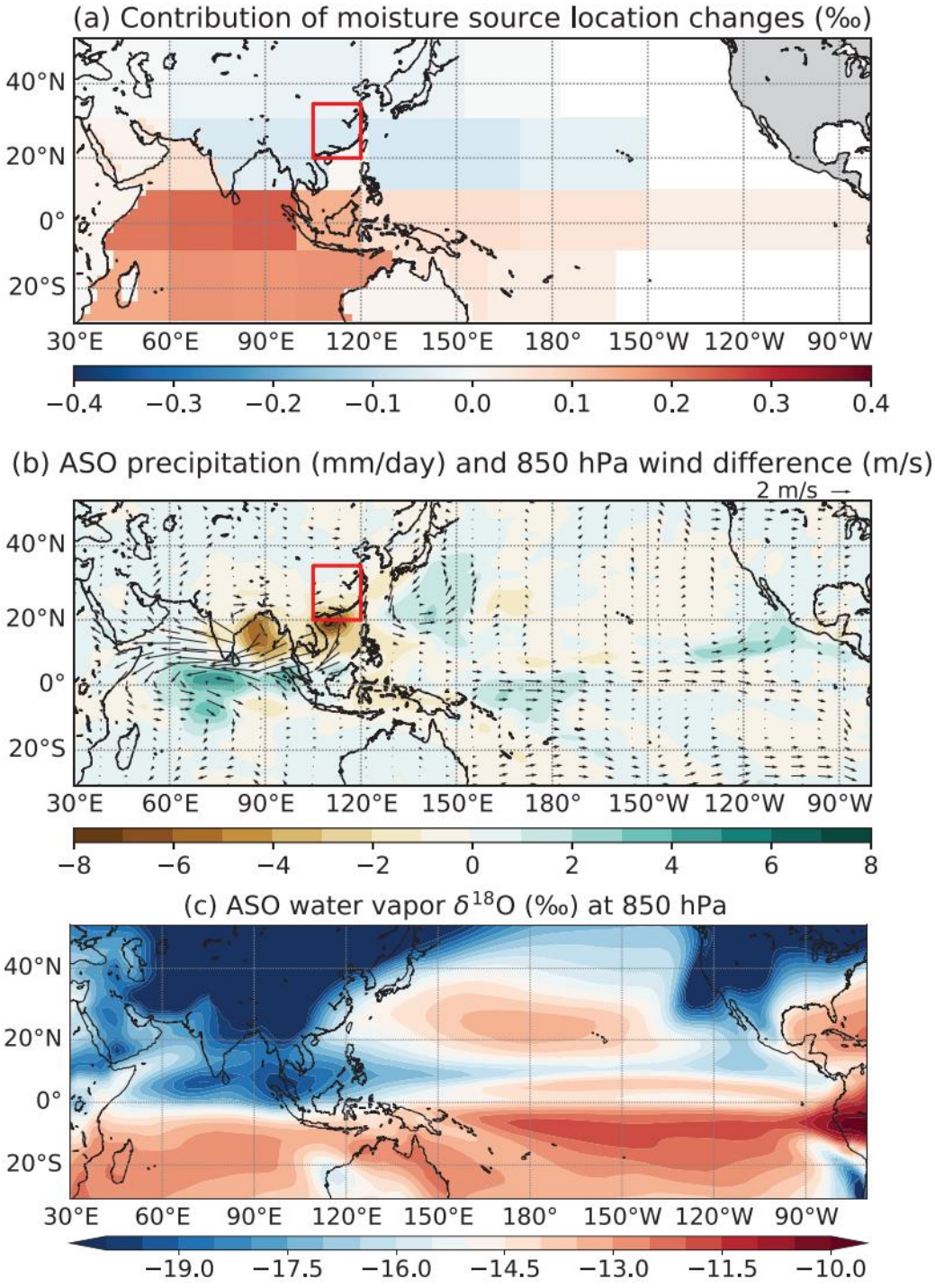

Figure 3. (a) Contribution of moisture source location changes to the interannual variability of East China $\delta^{18}O_P$ from tagged regions. (b) Difference of 850-hPa wind and precipitation in ASO between high and low $\delta^{18}O_P$ years of East China. (c) Climatological water vapor $\delta^{18}O$ at 850 hPa in ASO. The red rectangular is the defined East China region (20–35◦N, 105–120◦E).

8. 中国洞穴 $\delta^{18}O$ 记录的新见解及其古气候意义

翻译人：李海 Ultimate_LH@cug.edu.cn

*Liu, X., et al. (2020). New insights on Chinese cave δ18O records and their paleoclimatic significance. Earth-Science Reviews **207**: 103216.*

摘要：在过去的二十年中，石笋的氧同位素（$\delta^{18}O$）记录已被广泛用于研究古季风的演化。然而，将东部季风区的 $\delta^{18}O$ 记录作为东亚夏季风（EASM）降雨的指标已引起了激烈的争论。本次研究基于最近的研究进展，为中国洞穴 $\delta^{18}O$ 记录及其古气候意义提供了新的见解。本文的主要研究结论：（1）中国洞穴 $\delta^{18}O$ 记录不能反映整个中国东部季风的夏季降雨量的变化，这可以通过比较中国东部地区监测到的夏季降水量和综合的中国洞穴 $\delta^{18}O_{syn}$ 来证明。（2）由于对大尺度大气环流变化的敏感响应，中国洞穴 $\delta^{18}O$ 记录可以记录千年尺度的 EASM 事件。（3）在全新世早期（约 7 ka 之前），中国洞穴 $\delta^{18}O$ 记录与 EASM 降水（以华北降水为代表）之间的解耦关系归因于北部高纬度地区残余融冰的影响（4）当冰盖边界条件稳定且冰盖较小时（7 ka 之后），中国洞穴 $\delta^{18}O$ 与华北降水变化之间存在间接相关性。（5）在印度夏季风（ISM）的核心区域合成了横跨整个全新世的第一个连续石笋 $\delta^{18}O$ 记录。将 ISM 的代用指标与中国洞穴 $\delta^{18}O$ 记录进行比较后发现，在中国洞穴 $\delta^{18}O$ 主要记录热带季风和相关大尺度环流变化的信号。华北地区降水与热带季风（ISM）降水之间的耦合关系归因于下游环流对上游环流变化的响应，而它们之间的解耦关系则是由于北部高纬度冰盖减少北半球降水的影响所引起的。（6）由于季风“强度”的定义不精确，如果季风强度是由大气环流的变化定义的，我们建议将 $\delta^{18}O$ 洞穴用作 EASM 的替代。

Abstract In the last two decades, stalagmite oxygen isotope ($\delta^{18}O$) records have been widely used to study the evolution of the paleomonsoon. Nevertheless, interpreting cave $\delta^{18}O$ records in eastern monsoonal China as an indicator of East Asian summer monsoon (EASM) rainfall has been intensively debated. This study provides new insights into Chinese cave $\delta^{18}O$ records and their paleoclimatic significance, based on

recent research progress. The following points are highlighted: (1) Chinese cave $\delta^{18}O$ records do not reflect changes in summer rainfall throughout the whole of eastern monsoonal China, which is evident by comparing monitored summer rainfall amount in eastern China and an integrated Chinese cave $\delta^{18}O_{syn}$ proxy. (2) Chinese cave δ18O records can document millennial-scale EASM events, due to the sensitive response to large-scale atmospheric circulation changes. (3) During the early Holocene (before ~7 ka), a decoupled relationship between Chinese cave $\delta^{18}O$ records and EASM rainfall (as represented by precipitation in North China) is attributed to the reduction of rainfall in North China, due to the influence of remnant melting ice sheets in the northern high-latitude region. (4) When the ice sheet boundary conditions were stable and ice sheets were small (after ~7 ka), there is an indirect correlation between the Chinese cave $\delta^{18}O$ and rainfall changes in North China. (5) The first continuous speleothem $\delta^{18}O$ record spanning the entire Holocene is synthesized for the core region of the Indian summer monsoon (ISM)-domain. Comparison of this integrated ISM proxy with Chinese cave $\delta^{18}O$ records reveals that in China cave $\delta^{18}O$ is primarily a signal of changes in the tropical monsoon and related large-scale circulation. The coupled relationship between rainfall in North China and tropical monsoon (ISM) rainfall is attributed to the response of downstream circulation to changes in circulation upstream, while their decoupled relationship is due to the possible effects of northern high-latitude ice sheets on reducing rainfall in North China. (6) Due to the imprecise definition of monsoon "intensity", we suggest that cave $\delta^{18}O$ can be used as an EASM proxy, if monsoon intensity is defined by changes in atmospheric circulation.

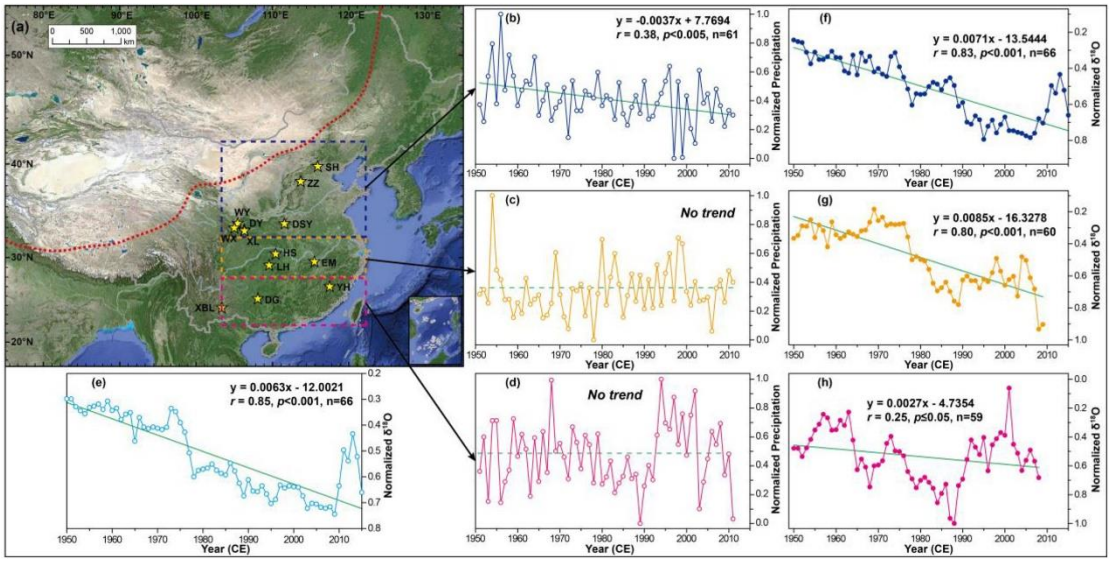

Fig. 1. (a) The dotted rectangular boundaries indicate the following areas: North China (43–32°N, 103–122°E), the Yangtze River Valley (YRV) (32–28°N, 103–122°E), and South China (28–22°N, 103–122°E). Variations of normalized summer (June to August) rainfall amount for North China (b), the YRV (c), and South China (d) during 1950–2011 are shown. (e) Variation of cave $\delta^{18}O_{syn}$ for the whole of eastern monsoonal China, shown for comparison. Variations of cave $\delta^{18}O_{syn}$ for North China (f), the YRV (g), and South China (h) are also plotted for comparison with the corresponding normalized precipitation records. Note that the linearly regressed summer rainfall of North China (b) shows a pronounced decreasing trend over the past ~60 yr, while no clear trends are evident for the YRV (c) and South China (d). In contrast, the variations of cave $\delta^{18}O_{syn}$ for the whole of eastern monsoonal China (e) and three sub-regions (f, g, and h) show linearly increasing trends over the past ~60 yr, passing a significance test. The trend of each time series was determined using the Mann-Kendall trend assessment and Ordinary Least Squares (OLS) regression methods .

9. 黄石公园北部热液系统的地质和热控制：高分辨率磁测的推论

翻译人：张伟杰 1312390861@qq.com

Bouligand, C. e M. A. Tivey, et al.. Geological and thermal control of the hydrothermal system in northern Yellowstone Lake: Inferences from high resolution magnetic surveys. Journal of Geophysical Research: Solid Earth, 2020-07-27.

摘要：作为黄石湖热液动力学研究的一部分，2016 年对黄石湖北部盆地进行了多尺度磁测量：一项综合的研究以期去描述地质和环境过程以及湖底热液活动之间的因果关系。多尺度磁测量获取了湖面磁数据、区域航磁数据和近底自治水下机器人磁数据。这项研究显示了东北部与西北部湖泊盆地的特征有明显的不同，东北部以区域低磁为特征的，中间间断有较强的局部低磁（许多这类地区具有较高的热液活动性），西北湖盆具有较高的活动性磁异常，没有明显的热液活动或间断磁低。在这两个区域的边界上，热流和磁值有一个较陡的梯度，这可能反映了目前活跃的约 20 公里长的鹰湾-湖酒店断裂带内的一个重要结构，该断裂带可能与约 2.08Ma 哈克贝利山脊火山口边缘有关。模拟表明，广阔的东北低磁区域反映了较浅的居里等温面和使岩石退磁的广泛的热液活动。湖的西岸展现出较高的磁异常，被认为是 West Thumb 流纹岩的上部单元的熔岩流的前缘。水下机器人的磁测结果表明，活动深孔热液喷口周边的磁化强度降低。我们推测，外区磁化强度的降低是由于热液增强了流纹岩的热液蚀变，而深孔热液喷口中心的喷出物以蒸汽为主蚀变较少。

ABSTRACT: A multi-scale magnetic survey of the northern basin of Yellowstone Lake was undertaken in 2016 as part of the Hydrothermal Dynamics of Yellowstone Lake Project (HD-YLAKE) — abroad research effort to characterize the cause-and-effect relationships between geologic and environmental processes and hydrothermal activity on the lake floor. The magnetic survey includes lake surface, regional aeromagnetic, and near-bottom autonomous underwater vehicle (AUV) data. The study reveals a strong contrast between the northeastern lake basin, characterized by a regional

magnetic low punctuated by stronger local magnetic lows, many of which host hydrothermal vent activity, and the northwestern lake basin with higher amplitude magnetic anomalies and no obvious hydrothermal activity or punctuated magnetic lows. The boundary between these two regions is marked by a steep gradient in heat flow and magnetic values, likely reflecting a significant structure within the currently active ~20-km-long Eagle Bay-Lake Hotel fault zone that may be related to the ca. 2.08-Ma Huckleberry Ridge caldera rim. Modeling suggests that the broad northeastern magnetic low reflects both a shallower Curie isotherm and widespread hydrothermal activity that has demagnetized the rock. Along the western lake shoreline are sinuous-shaped, high-amplitude magnetic anomaly highs, interpreted as lava flow fronts of upper units of the West Thumb rhyolite. The AUV magnetic survey shows decreased magnetization at the periphery of the active Deep Hole hydrothermal vent. We postulate that lower magnetization in the outer zone results from enhanced hydrothermal alteration of rhyolite by hydrothermal condensates while the vapor-dominated center of the vent is less altered.

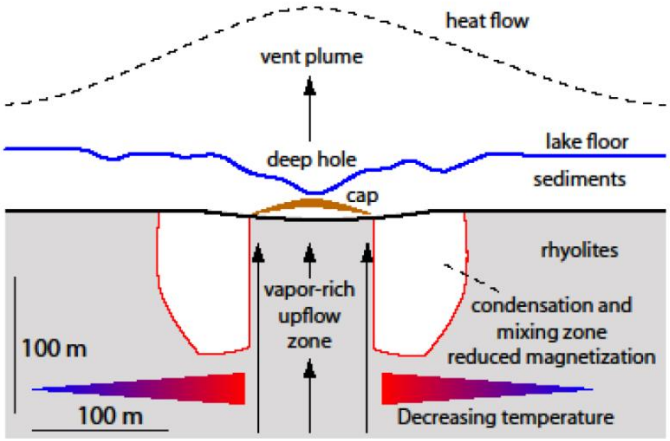

Figure 1. Schematic diagram showing a cross-section of the Deep Hole hydrothermal site with a central upflow zone of vapor-dominated fluid where alteration of magnetic minerals is limited compared to the surrounding zones of condensation/mixing where hydrothermal alteration is enhanced and results in decreased magnetization. A semi-impermeable cap composed of kaolinite-boehmite altered mud overlies the upflow zone within the sediments.